An NMR Determination of the Physiological Water Distribution in Wood during Drying*

R. S. MENON,† *Forintek Canada Corp. Western Laboratory, 6620 N.W. Marine Drive, Vancouver, B.C., V6T 1X2, Canada* A. L. MACKAY, *Department of Physics, University of British Columbia, Vancouver, B. C., V6T 2A6, Canada,* J. R. T. HAILEY,‡ *Forintek Canada Corp. Western Laboratory, 6620 N.W. Marine Drive, Vancouver, B.C., V6T 1X2, Canada,* M. BLOOM, *Department of Physics, University of British Columbia, Vancouver, B.C., V6T 2A6, Canada,* A. E. BURGESS, *Department of Radiology, University of British Columbia, Vancouver, B. C., V6T 1W5, Canada* and J. S. SWANSON, *Forintek Canada Corp. Western Laboratory, 6620 N.W. Marine Drive, Vancouver, B.C., V6T 1X2, Canada*

Synopsis

Proton magnetic resonance has been used to study water in Douglas fir and western red cedar. The free induction decay, when combined with a knowledge of chemical composition of the wood, gives an accurate measure of the absolute moisture content. Spin-lattice relaxation was found to be significantly different for the two species. In sapwood, three distinct spin–spin relaxation times, T_2, were measured and assigned, with the help of anatomical data, to water in and on the cell wall, water in the ray and latewood tracheid lumens, and water in the earlywood tracheid lumens. This T_2 behavior was explained by a model in which free water in a void exchanges with a small fraction of bound water on the lumen surface. The three T_2's were almost independent of moisture content, suggesting physically separate compartments. The behavior of the three water components during drying was studied. The fiber saturation point could be determined from a single T_2 measurement on a green sapwood sample. Magnetic resonance imaging of logs was investigated.

INTRODUCTION

The distribution and interactions of water in wood are of great importance in the commercial utilization of wood. Thus, the characterization of this water is essential for the sophisticated control of the chemical and structural properties of wood.[1]

Proton nuclear magnetic resonance (^{1}H-NMR) is not a new tool in the understanding of wood-water interactions[2,3] or water–cellulose interactions.[4] Pulsed NMR has been used to determine the moisture content (MC) of wood relative to a known standard,[5] but no attempt has been made to directly

* Work supported by the Canadian Forestry Service and the Natural Sciences and Engineering Research Council of Canada.

† On intersession leave from University of Alberta.

‡ Author to whom requests for reprints should be addressed.

Journal of Applied Polymer Science, Vol. 33, 1141–1155 (1987)
 CCC 0021-8995/87/041141-15$04.00

relate the MC determined by NMR to that determined by the normal oven-dry method defined by Tappi Standard T 12 OS-75.

NMR spin-lattice (T_1) and spin–spin (T_2) relaxation times have also been used[6–8] in a physiological attempt to locate water in wood. However, incomplete and relatively unsophisticated data reductions have prevented these researchers from reaching simple conclusions.

In this study, a comprehensive investigation of the ^{1}H-NMR signal (FID intensity, T_1 and T_2) from water in Douglas fir [*Pseudotsuga menziesii* (Mirb.) Franco], henceforth called fir, and western red cedar (*Thuja plicata* Donn) was made. The behavior of three distinct mobile water components was studied during stepwise oven drying in order to identify where these components were physically located and to learn about the wood drying process. Anatomical data were obtained to determine the physical locations of the water. The work was done on both heartwood and sapwood. The NMR characterization of this water also allows optimization of parameters for imaging different types of water in logs by magnetic resonance imaging (MRI), which is being done in parallel with this work.

MATERIALS AND METHODS

Samples

Three rectangular cedar sapwood samples were cut from a 1 cm thick transverse slice of a green log. The resulting sample blocks measured approximately 1 × 0.55 × 0.55 cm with the long axis of the block parallel to the longitudinal tracheids in the wood. Each sample was placed at the bottom of a 18 cm long, 10 mm o.d. NMR sample tube, and a 17 cm long teflon dowel, 8 mm in diameter, was then inserted just above the wood in order to minimize the air space with which the wood could equilibriate. A tight fitting plastic cap was used to seal the tube.

Similarly, two samples each of cedar heartwood, fir sapwood, and fir heartwood were prepared. The cedar sapwood samples were taken from circumferentially adjacent positions and seemed uniform. The heartwood samples were adjacent to one another in the logs. The fir samples were chosen from opposite sides of the log, and one (sample F_1) had a larger percentage of latewood than the other (sample F_2).

The stepwise drying was only done on the five sapwood pieces. After each NMR measurement, the sample was weighed while in the sample tube with the dowel and cap on, and then oven-dried at 70°C and under 760 mm of vacuum without the cap. The tubes were then removed from the vacuum oven, recapped, and allowed to reequilibriate for 2 h, while monitoring T_1, before commencing the next NMR measurement. It had previously been determined that 10 min of drying under the above conditions removed 15% of the water by weight of dry wood. In this study, the MC of wood is always given by weight of the dry wood.

All the wood was eventually oven-dried until no weight change occurred to determine the MC at each point in the experiment. Density measurements were made on each of the sapwood samples using the saturated and oven-dry sample weights.

NMR Measurements

The ^{1}H-NMR measurements were made on a Bruker SXP 4-100 NMR spectrometer, operating at 90 MHz. The signal was acquired using a Nicolet 1090AR dual-channel digital oscilloscope and successive scans accumulated by an Intel 8080A based microcomputer. The 90° pulse length was 1.5 μs and the receiver dead-time was 8 μs during which the receiver was saturated by the 90° RF pulse. Free induction decays (FIDs) were measured by accumulating 50 scans with a 90°_x pulse and subtracting 50 scans obtained with a 90°_{-x} pulse. This reduced spurious signals due to coherent background noise and also reduced the effect of the intense RF pulse on the receiver electronics. The FIDs were collected with a 0.5 μs dwell time for 4096 points and stored on disk for future reference and plotting. Digitization was started halfway through the pulse, since this is the effective starting time for the time evolution of the spin system.[9] The time between 90° pulses was 4 s, which allowed the magnetization to return to equilibrium.

The T_2 measurements were made using the Meiboom–Gill[10] modification of the Carr–Purcell[11] sequence. This pulse sequence, known as the CPMG sequence, is briefly annotated by 90°–$\tau/2$–$(180^\circ$–τ–$)_n$–τ_r and consisted of a 90° pulse followed by n repeated 180° pulses, at a τ value of 200 μs in this experiment. The CPMG sequence lasted 405 ms and the entire sequence was repeated with a recycle time τ_r of 4 s. One thousand scans were collected and averaged.

For the T_1 measurement in heartwood, an inversion recovery sequence was used. This consisted of a 180° pulse applied at a time τ before every second 90° pulse corresponding to the sequence (0°–τ–90°–τ_r–180°–τ–90°–τ_r). The FID signal each first (second) 90° pulse was added (subtracted) from the accumulated signal in memory. For heartwood, 21 τ values were used. In sapwood, a 180°–τ–90° seqence was used, and the value of τ required to zero the signal in the x–y plane noted. This measured a weighted average value of T_1, and was used to monitor the return to equilibrium of the sample after heating and pumping on the sapwood samples. Typically, the value of T_1 stabilized in 1 h. The recycle time here was also 4 s, chosen to exceed the longest T_1 by at least $6 \times T_1$.

All samples were at 24°C at the beginning of a NMR measurement, but the CPMG sequence caused a 5°C rise in the sample temperature over the 67 min data acquisition time. There was no evidence that the T_2's had a strong temperature dependence.

Finally, it should be noted that the main magnetic field was perpendicular to the tracheid axis and samples were always replaced with the same orientation in the probe whenever possible. This reduced variations in the orientation dependence of the NMR signal on the direction of the wood grain.[12]

Anatomical Methods

Samples of each fir (one from each side of the tree) and cedar sapwood were taken adjacent to the samples used for the spectroscopic work. They were examined using a Hitachi Model S-500 scanning electron microscope (SEM) located at the Agriculture Canada Vancouver Research Station. The samples were sputter coated with gold. The power was varied between 10 and 20 kV

depending on the sample view. Photomicrographs at 25 power magnification were taken for the cross, radial, and tangential sections of each sample. Using a 200 times magnification, the earlywood, latewood, and ray parenchyma cell diameters and cell wall thicknesses were measured. The volumes occupied by each cell type were determined.

RESULTS

Figure 1 shows a series of FIDs for cedar sapwood at different MCs. All FIDs could be separated unambiguously into a rapidly decaying component ($T_2^* < 100$ μs) and a slowly decaying component ($T_2^* > 200$ μs). At short times the rapidly decaying component corresponds to relatively immobile protons in the wood's structural components whose contribution was not expected to change during drying. Therefore, the intensities of all CPMG data

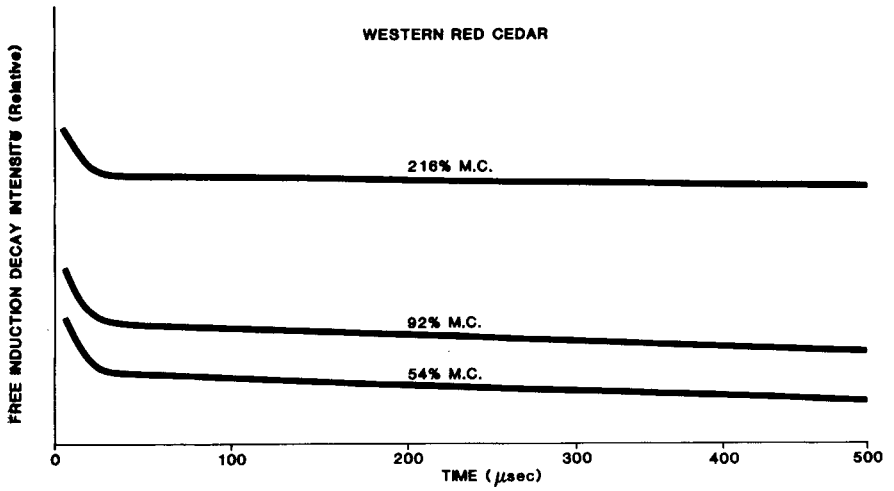

Fig. 1. The ^{1}H-NMR free induction decay for western red cedar sapwood at three moisture contents: 216, 92, 54%.

TABLE I
Comparison of Moisture Content for Cedar Obtained from the Free Induction Decay with That Obtained by Oven Drying (% Dry Wt Wood)

Cedar sapwood MC (%)		Cedar heartwood MC (%)	
NMR	Oven dry	NMR	Oven dry
211 ± 10	216 ± 1	19 ± 1	20
175	163	25	25
145	142		
120	111		
99	92		
76 ± 5	72		
57	54		
38	38		
33	31		
22 ± 1	21		
5	9		

TABLE II
Comparison of Moisture Content for Fir Obtained from the FID with That Obtained by Oven Drying

Fir sapwood MC (%)		Fir heartwood	
NMR	Oven dry	NMR	Oven dry
103 ± 10	105 ± 1	35	22
99	92	22	20
73	77		
73	73		
66	59		
47	50		
3 ±1	5		

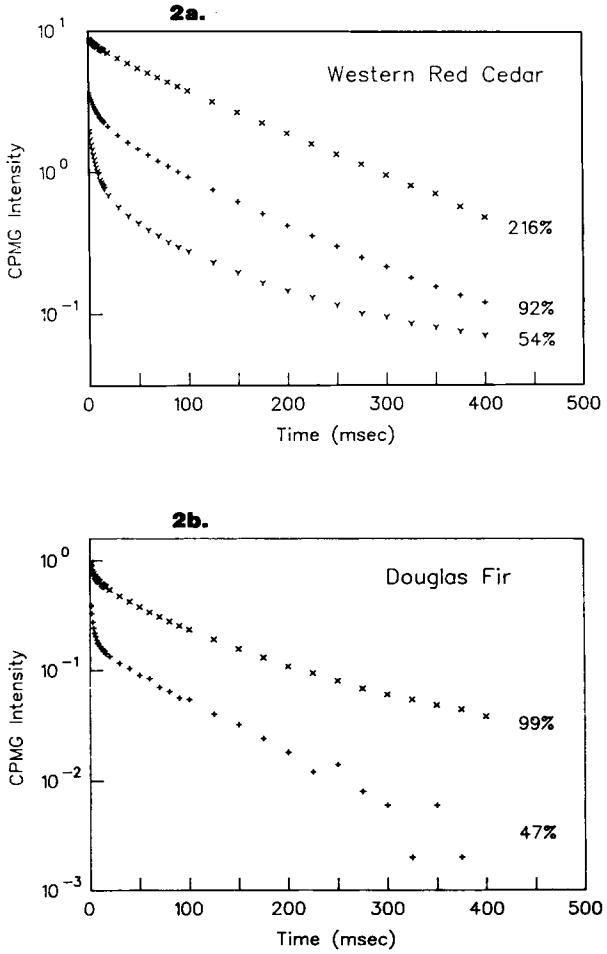

Fig. 2. Carr–Purcell–Meiboom–Gill (CPMG) decay curves for (a) western red cedar and (b) Douglas fir.

TABLE III

T_1 Values, T_2 Values, and Water Content Corresponding to Each T_2 Component for a Range of Moisture Contents for Western Red Cedar Sapwood

MC (%) oven dry	T_2 (ms)			T_1 (ms)	Water content (%) of dry wood volume		
	Fast	Medium	Slow		Fast	Medium	Slow
216	7.4 ± 3	42 ± 2	148 ± 5	405 ± 5	7.0 ± .5	9.6 ± 1	65.1 ± 1
163	8.3	46	150	405	8.8	8.8	43.9
142	8.5	47	144	360	9.8	11.6	32.6
111	7.6	49	142	310	11.0	9.9	22.6
92	7.2	49	154	270	11.5	10.2	14.1
72	5.7	28	127	220	11.0	7.5	11.7
54	5.3	30	179	170	11.0	5.3	4.8
38	4.1	14	468	140	10.2	3.6	1.7
31	4.1	23	745	110	11.0	1.7	0.8
21	3.7	107	—	99	8.5	0.9	0
9	1.5	—	—	170	3.9	0	0

TABLE IV

T_1 Values, T_2 Values, and Water Content Corresponding to Each T_2 Component for a Number of Moisture Contents for Douglas Fir Sapwood

MC (%) oven dry	T_2 (ms)			T_1 (ms)	Water content (%) of dry wood volume		
	Fast	Medium	Slow		Fast	Medium	Slow
103	2.9 ± .3	49 ± 2	184 ± 2	120	12.3 ± .5	16 ± 1	14.0 ± 1
99	2.4	37	162	110	10.5	10.5	11.5
73	2.4	15	100	90	9.2	4.4	11.6
73	2.5	17	103	86	9.1	4.1	11.1
66	2.4	13	99	77	8.8	3.3	10.1
47	2.5	17	96	60	8.9	2.4	5.1

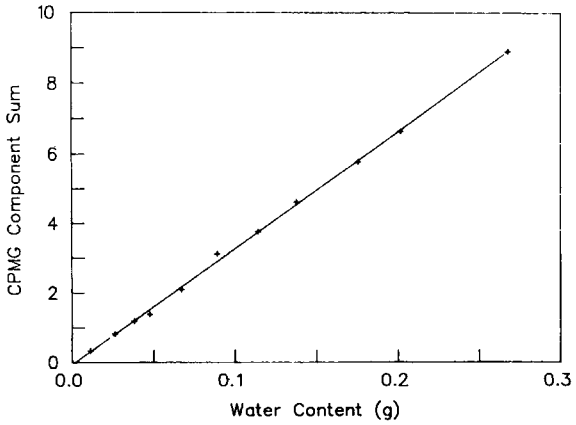

Fig. 3. A plot of the sum of the amplitudes of the three components of T_2 as a function of moisture content for western red cedar. The straight line represents a linear fit of the points.

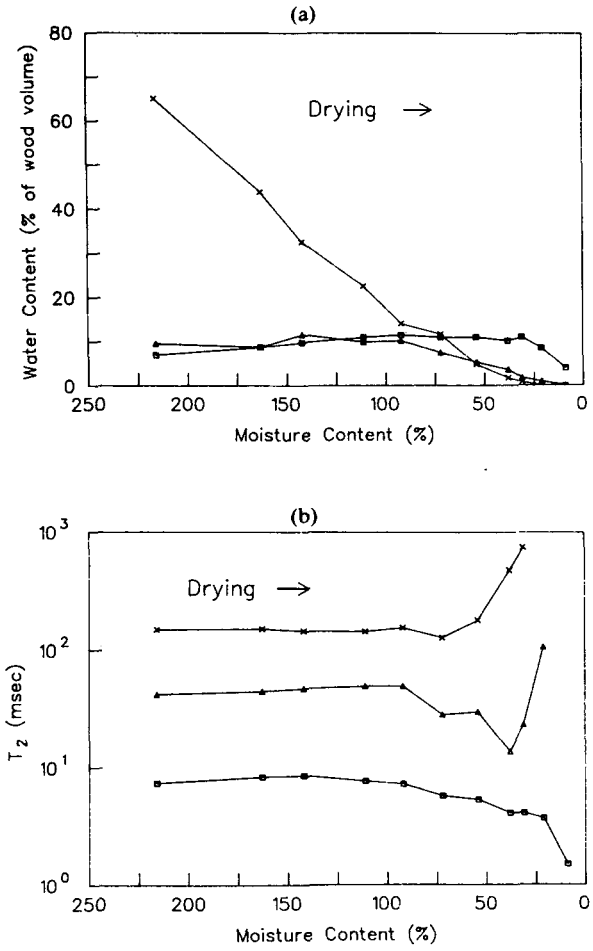

Fig. 4. Behavior of (a) CPMG component populations (% volume of green wood) and (b) T_2 values (ms) as a function of moisture content in cedar sapwood.

were normalized using the solid proton signal from the FID at each MC. In practice, the normalization factor for each sample was constant to within a few percent. The slowly decaying component arising from the mobile protons should be a superposition of exponentials but the shape for times longer than 2 ms is strongly influenced by magnet inhomogeneity, necessitating the use of the CPMG sequence to measure the T_2 decay. The zero time intercept of the solid and mobile components is proportional to the number of protons giving rise to each. The moisture in the wood determined by the FID (with the corrections described below) is compared with the MC from the oven-dry method for cedar and fir in Tables I and II, respectively. Results are presented for both sapwood and heartwood.

In Figures 2(a) and 2(b), representative CPMG curves for two hydration levels are shown for cedar and fir sapwood. On a semilogarithmic plot of the CPMG decay with an expanded timescale, three distinct components become apparent on visual inspection. These are all due to relatively mobile water.

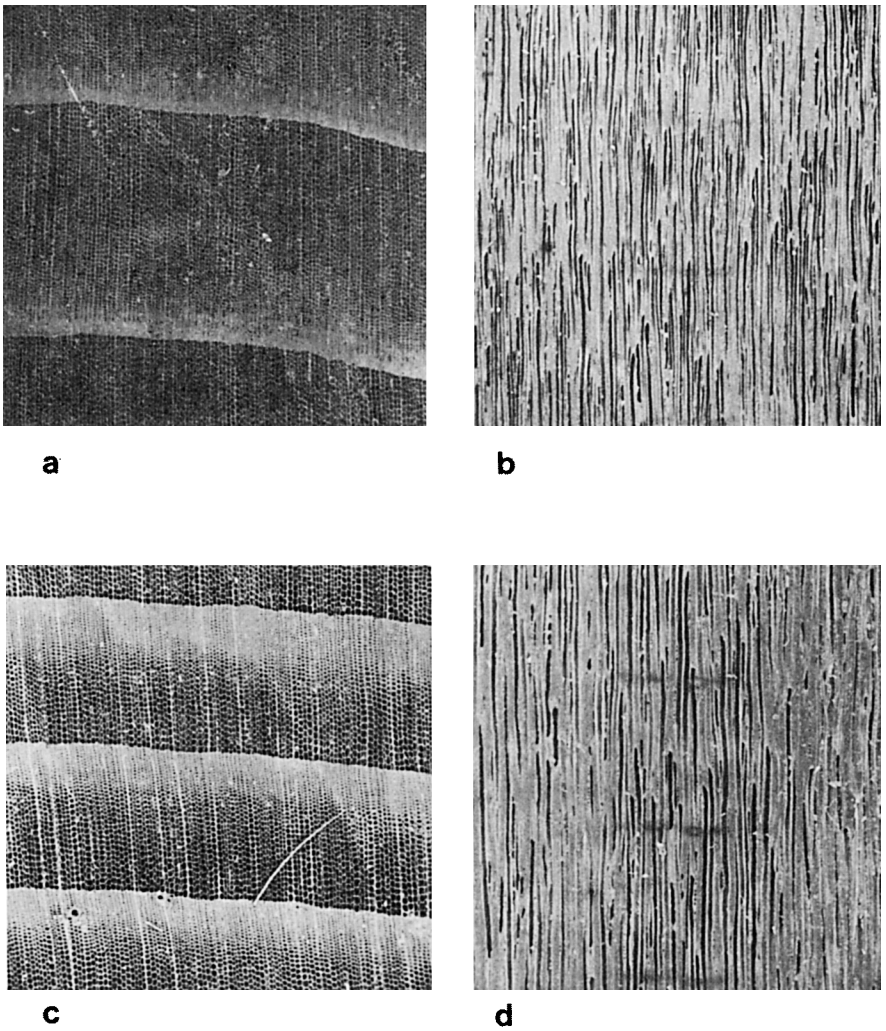

Fig. 5. Scanning electron photomicrographs of cross and tangential sections of western red cedar (a, b) and Douglas fir sapwood (c, d).

The CPMG data was collected until the signal was down to less than 1% of the initial amplitude. This combined with a good signal to noise ratio has allowed us to see the third component that others have missed.[6,7] Using the methods outlined in the discussion, the three components of the CPMG decay were separated. These are tabulated in Table III for cedar sapwood and in Table IV for fir sapwood. The weighted average T_1 values for the sapwood samples are also presented in these tables. It should be noted that the spin lattice relaxation curves were nonexponential. To demonstrate the accuracy of the CPMG analysis, the sum of the amplitudes of the three water components is plotted versus MC in Figure 3. The data of Table III is plotted in Figures 4(a) and 4(b) to emphasize the individuality of the three water components.

Figure 5 shows the photomicrographs of the wood samples used, and Table V lists the various anatomical data measured from these microsections.

TABLE V
Specific Gravity and Cell Dimensions for Western Red Cedar and Douglas Fir Sapwood

	Cedar	Douglas fir	
Specific gravity	0.354[a]	0.704[b]	0.526[c]
Earlywood tracheids			
Cell diameter (μm)	29 ± 10	41[d] ± 10	
Cell wall thickness (μm)	2	3	
Cell lumen diameter (μm)	25	35	
% Lumen volume[e]	56	33	
% Earlywood volume	76	55	
Latewood tracheids			
Cell diameter (μm)	13 ± 5	15 ± 5	
Cell wall thickness (μm)	4	5	
Cell lumen diameter (μm)	5	5	
% Lumen volume	2	4	
% Latewood volume	14	37	
Ray parenchyma (Ray)			
Cell diameter (μm)	12 ± 3	13 ± 4	
Cell wall thickness (μm)	3	3	
Cell lumen diameter (μm)	6	7	
% Lumen volume	3	2	
% Ray volume	10	8	

[a] Three-sample average.
[b] Fir F_1 compression wood.
[c] Fir F_2 normal wood.
[d] Anatomical measurements for F_2 only.
[e] Based on green dimensions.

DISCUSSION

Moisture Content

In order to use NMR to determine the MC of wood without using a reference standard, the proton density of wood and water must be calculated. Since the NMR signal is proportional to proton density, the MC may be obtained from the FID using the equation:

$$\text{MC} = \frac{M(0)}{S(0) - M(0)} \times \frac{\rho_H(\text{wood})}{\rho_H(\text{water})} \times 100\% \quad (1)$$

where $M(0)$ and $S(0)$ are the zero time intercepts of the mobile and total signal component of the FID and the proton density in terms of the number of protons per gram is denoted by ρ_H. Using the values of ρ_H appropriate to cellulose and lignin for western red cedar[13] and Douglas fir,[14] the modifying ratio $\rho_H(\text{wood})/\rho_H(\text{water})$ in eq. (1) becomes 0.549 for cedar and 0.538 for fir. This suggests that the proton density in cedar is roughly 2% higher than in fir. The above procedure represents the first known attempt to reconcile the MC measured directly from the FID with the MC from the oven-dry method. The agreement of the two methods puts an upper limit on the difference in proton density between heartwood and sapwood of the same species. NMR thus

provides a very simple, fast, nondestructive way of measuring the MC of wood, with eq. (1) holding over all physiological hydrations, in direct contrast to the complex formulations of previous workers.[15] In the above, it has been assumed that the percentage of extracts is small and makes a negligible contribution to the NMR signal. From the data in Tables I and II, one may estimate from the systematic error that the extractives, if present, contribute less than 3% of the signals. It has also been assumed that, in terms of proton density, wood can be considered to be made up of only cellulose and lignin.

Relaxation Measurements

As discussed earlier, the magnet linewidth of approximately 80 Hz precludes the determination of T_2 from the FID. The 180° pulse in the CPMG sequence reverses the phase of the magnetization, thus giving rise to a spin echo in which the influence of chemical shifts and magnetic inhomogeneities are eliminated. The 180° pulse does not change the effects of dipolar or other second-order interactions. Thus, the "true" T_2 of the nondipolar broadened line can be measured. It was found that, for τ in the range 200 μs–20 ms, the echo envelopes were the same, showing that there are no slow motions in the system with correlation times in this range. The implications for imaging on present day magnetic resonance imaging (MRI) machines will be discussed later.

At all drying stages it was possible to separate the CPMG decay curve unambiguously into three exponential components. It should be noted that quantitative separation of superimposed exponentials is nontrivial. The common procedure of successively fitting to two or more straight lines on a semilogarithmic plot is hopelessly inaccurate because it places too much significance on the relatively noisy data at longer times. In the present study, the nonlinear functional minimization program MINUIT[16] was used to fit the data to

$$Y = A\exp(-Bt) + C\exp(-Dt) + E\exp(-Ft) \qquad (2)$$

where B, D, and F are the inverses of the three T_2 values for the three components and A, C, and E are their respective populations. All CPMG data points were assumed to have equal variance, and initial parameter values were estimated from visual inspection of the decay curves. Confidence limits of 68% were obtained for the fitted parameters. Equation (2) produced the best fits to the data. Two exponential fits gave larger mean square deviation and four exponential fits did not converge well. The fact that the three time constants differed considerably in magnitude helped in separating the exponentials. When the sum of the three amplitudes was plotted versus measured water content in a sample (see Fig. 3), the deviation from a linear fit (CPMG sum = 33.56 × water content (in g) − 0.0722) was less than 0.2% over the entire MC range. This strongly supports the claim that the sum of the three amplitudes represents the total amount of water in a sample.

The fact that the T_2 values do not change with MC is also strong evidence for the validity of the calculated populations. A small change in T_2 would otherwise lead to a large change in calculated population. More important, since the T_2 of each compartment is constant over a large hydration range, it

is possible to state that the three types of compartments are physically separate with little exchange between them.

The graph of population versus MC for cedar sapwood shows different behavior for each component [Fig. 4(a)]. Starting from large hydrations, water is initially lost from the slowest decaying T_2 component, while the other two remain relatively unaffected. At 100% MC, water begins to be removed from the medium component, but at a slower rate than from the slowest component. By $\simeq$ 31% MC, the slow T_2 component is completely gone and water begins to leave the fast T_2 component. Not until $\simeq$ 10% MC is the medium component completely removed. The behavior of fir through drying is qualitatively similar to that of cedar.

Assignment and Interpretation of the CPMG Components

On the basis of the volume occupied by the three components and the measured anatomical data, the three components can be assigned as follows. The fast T_2 component is identified with water in and on the cell wall fibrils. The medium component is assigned to the water in the ray and latewood tracheid lumens and the long component to the water in the earlywood tracheid lumens.

Assuming that the mechanism for T_2 is exchanged with surface hydration water on the lumen walls, one can explain the relative magnitudes of the T_2's. Water in the cell wall is considered bound on and between cellulose fibers in the cell wall, the vast majority of water being in the S2 layer of the cell wall. Water in the rays and latewood tracheid lumens has a higher surface area to volume ratio than in the earlywood tracheid lumens. This larger surface area provides for more efficient relaxation, resulting in a shorter T_2. As a model, we may write

$$\frac{1}{T_2(\text{meas})} = \frac{f}{T_2(\text{bound})} + \frac{1-f}{T_2(\text{free})} \tag{3}$$

where T_2(meas) is the measured T_2 value of the water in a void, f is the fraction of water bound on the void surface and, with the appropriate ion concentration,[17] T_2 (free) $\simeq$ 1.5 s. Assuming that T_2(bound) $\simeq$ T_2(cell wall) $\simeq$ 7.4 ms for cedar, the fraction f of surface states may be obtained from eq. (3) using the measured T_2.

When calculating average sizes from micrographs for comparison with NMR data, it must be noted that the NMR signal is proportional to the number of nuclei contributing to it. Therefore, an average size calculation should be weighted by the structure volume. For wood cells, which we treat as infinite cylinders, this means that the weighting function for average diameter calculations is the square of the lumen radius.

For cedar sapwood, the weighted ratio of surface to volume is 3.9 times higher in rays than in earlywood tracheids and 2.6 times higher in latewood tracheids than in earlywood tracheids. Due to the distribution of cell sizes, the standard deviation in these numbers is about 40%. From the cedar sapwood NMR T_2 data for moisture contents from 38 to 216%, the corresponding ratio of surface bound water fractions was 3.4 with a standard error of 0.3. This is

strong evidence for the validity of the model used to explain the measured T_2 values in the cell walls.

For Douglas fir sapwood, the weighted ratio of surface area to volume is about 5 times higher in rays than in earlywood trancheids and about 4 times higher in latewood tracheids than in earlywood tracheids. The standard deviations in these numbers is about 60%, indicating a larger distribution of cell sizes in fir than in cedar. The fir sapwood NMR data for moisture contents from 47 to 103% yielded a corresponding surface to volume ratio of 6.5 with a standard error of 1.5.

If τ_b is the correlation time of a water molecule (assuming exponential time decay) on the bound surface site and τ_f the correlation time of free water, we can derive the equations for T_1 and T_2[18] using $\tau_b \gg \omega_0^{-1}$ and $\tau_f \ll \omega_0^{-1}$, where ω_0 is the resonance angular frequency. These equations are

$$T_1^{-1} = f(12/5)\left(A/\omega_0^2\tau_b\right) + (1 - f)6A\tau_f$$

$$T_2^{-1} = f(9/5)(A\tau_b) + (1 - f)6A\tau_f \tag{4}$$

$$A = \gamma^2\mu^2/r^6 \text{ s}^{-2} = 8.7 \times 10^9 \text{ s}^{-2}$$

where γ is the proton gyromagnetic ratio (2.675×10^4 s^{-1} G^{-1}), μ is the magnetic moment (1.41×10^{-8} erg G^{-1}). Because $\tau_b \gg \tau_f$, T_2 is determined by the bound fraction, even for very small values of f. Since the ratio of surface area to volume of a cylinder depends on the inverse of the radius, T_2 remains constant as the water level drops in the tracheid. However, since the bottom of a tracheid is tapered, the surface area to volume ratio is higher at the bottom by roughly 1.5, so that T_2 should drop proportionately as the water level drops to the tapered part. This appears to be the case until an anomalous rise occurs in the T_2 of the two void volumes at very low hydrations. A possible explanation of this is presented later.

The cedar heartwood CPMG data could also be separated into more than one component; however, the T_2's were considerably shorter. At this stage it can only be hypothesized that the smaller cell sizes and more rigid structure of the heartwood are responsible for the shorter T_2 values. The T_1 decay in heartwood consisted of two distinct components of the same relative proportions at every point along the first 1 ms of the FID, including the solid signal from protons in cellulose. Thus, the solid signal appears to have the same T_1's as all the mobile components in heartwood, indicating the presence of spin diffusion processes between the solid wood and the water in a time of order T_1. A detailed T_1 analysis for sapwood was not carried out, but the average T_1 of the heartwood is within 10% of the average T_1 of the sapwood in both species for the same MC. This tends to suggest that the T_1 mechanism is to a first approximation, independent of the cell wall structure. Equation (4) predicts this, since the mobile fraction with the correlation time τ_f is the larger determining factor for T_1. Of course, the interpretation of spin lattice relaxation here is complicated by the coupling to the solid protons.

Another interesting feature of Figure 4(a) is the 40% increase in the amount of water in the fast component as the MC initially decreases. That this

represents a real increase in the amount of water in the cell wall is physiologically impossible, since the water in this component at 216% MC corresponds to the maximum volume available in the cell wall for hydration. One explanation is that as the water level decreases in the tracheids, capillary action, and water vapor produce a water layer on the surface of the lumen. This water does not exchange with the cell free water, as it has little contact with the free water and consequently relaxes with a T_2 similar to that of the cell wall water. When there is no free water left in the lumen, the amount of water in the fast component returns to the amount that should be in the cell wall. This is only a qualitative explanation, but seems plausible based on calculations of capillary tension and vapor pressure.[19] The population changes are not sudden and their shapes are typical of compartments in equilibrium. Since there are connections known as pits between the rays and tracheids as well as between the tracheids, completely neglecting mixing between compartments is not realistic. But, based on the apparent lack of slow motions in the system, it may be that mainly water vapor equilibration and not water diffusion occurs between the voids.[19]

As the MC decreases the T_2 of the fast component drops smoothly and continuously. This may be due to conformational changes in the cell wall constituents which occur as water is removed from the walls.[20]

The reason for the increase in the T_2 in the voids when they are almost empty is unknown. The populations of the components decrease monotonically, giving credibility to the curve fitting process and the validity of these T_2 values. It is conceivable that water in the tapered ends of the tracheids forms droplets over or in the aspirated pits and that this water behaves much like free water. Since the strands of the margo in a pit do not form a solid surface, the relaxation process in these pits may be slower.

One of the most important features of Figure 4(a) is that it sheds new light on the fiber saturation point (FSP). The original definition of the FSP by Tiemann[21] was the MC at which the cell walls are saturated with bound water, with no free water in the lumens. Others[22] have variously interpreted the FSP as the MC at which discontinuities in physical properties of the wood such as shrinkage, strength, or conductivity change. Two points may be noted from this figure.

First, assuming the cell wall to be full of water in a saturated sapwood sample, the three-component analysis tells how much water is in the cell wall and hence immediately defines Tiemann's FSP. This assumes water does not leave the cell wall until the voids are empty. This brings the second feature out, because all the water has not left the ray and tracheid compartments when water begins to leave the cell wall at about 31% MC. Water is not gone from the void volume until the water is down to 9% by weight. This NMR data indicates that the concept of FSP should be reevaluated.

The data on fir sapwood gives some insight into the differences between earlywood and latewood. The sample which had a higher percentage of latewood (thicker cell walls and smaller cell diameters typify latewood) had a 60% shorter T_2 for the cell wall component. Fir in general has a cell wall T_2 which is about 3.5 times shorter than that for cedar. As a result, the T_2 values in the cell voids are shorter, due to the effect of surface states on the T_2 of the water in the lumens. Otherwise, behavior of the T_2's and populations during

drying is similar to cedar sapwood. The spin lattice relaxation in fir heartwood has two distinct components, but the ratios of the two are slightly different than in cedar.

Therefore, NMR appears to be able to distinguish different species based on the T_2's of their components. It is sensitive to differences in hydration as well as to cell size and cell wall thickness.

Imaging of Wood by NMR

One aim of this study was to identify characteristics of water in wood that can be nondestructively imaged; the eventual goal being to use an MRI machine to obtain a spatial map of wood properties for an entire log. Equivalent measurements on an NMR spectrometer would take much longer.

Unfortunately, imaging machines have considerably more limitations than spectrometers. The 90° RF pulses are typically several milliseconds long, which limits the pulse repetition rate for a sequence such as the CPMG. This also limits the shortest T_2 components which may be seen. Most MRI machines do not collect multiple echos, so that a true spin–spin relaxation decay curve cannot be obtained. Also, a CPMG sequence with $\tau = 20$ ms may not yield the same T_2's as those in a spectrometer since the value of τ chosen determines what types of molecular motions may be seen. In wood, this does not appear to be a problem, based on measurements to date. Work in progress at UBC shall attempt to circumvent these limitations and to spatially identify at least the two longer components in the sapwood of logs.

CONCLUSIONS

Water is an excellent probe of wood because it is sensitive to the wood ultrastructure. It has been shown that the volume occupied by water in different environments can be identified by NMR and is consistent with the measured anatomical data. The water T_2 behavior may be accounted for by the exchange of free water with bound water on the cell lumen walls. The T_2 data in the voids is consistent with the ratio of the surface area to volume of the rays and tracheid lumens. The T_2 of water is species-dependent in the cell wall, as well as between the earlywood and the latewood. NMR can be used as a nondestructive determination of the FSP from a green sample's CPMG decay curve. Furthermore, the FSP derived from NMR is a direct measurement of the cell wall water content and therefore unambiguous. Detailed behavior of the mechanism by which water leaves wood during drying has been presented. Using the NMR data collected, work is now underway to image water in whole logs. The advantages of such a nondestructive technique could revolutionize lumber utilization.

The authors gratefully acknowledge the other members of the discussion group on wood, Dr. Iain Taylor of the Department of Botany, University of British Columbia, and Dr. Frank Volke of the Department of Physics at Karl Marx University in Leipzig for providing insight as only such a diverse group can. One of the authors (R. M.) also wishes to thank Dr. Ian Booth for comments made during the writing of this paper. The authors gratefully acknowledge Josephine Gonzales, Forintek Canada Corp. for acquiring the scanning electron micrographs.

References

1. C. Skaar, *Water in Wood*, Syracuse University Press, Syracuse, NY, 1972.
2. A. Odajima, *J. Phys. Soc. Jpn.*, **14**, 308–312 (1959).
3. T. Swanson, E. O. Stejskal, and H. Tarkow, *Tappi*, **45**, 929–932 (1962).
4. E. Hsi, G. J. Vogt, and R. G. Bryant, *J. Colloid Interface Sci.*, **70**, 338–345 (1979).
5. A. R. Sharp, M. T. Riggin, R. Kaiser, and M. H. Schneider, *Wood Fibre Sci.*, **10**, 74–81 (1978).
6. E. Hsi, R. Hossfeld, and R. G. Bryant, *J. Colloid Interface Sci.*, **62**, 389–395 (1977).
7. M. T. Riggin, A. R. Sharp, R. Kaiser, and M. H. Schneider, *J. Appl. Polym. Sci.*, **23**, 3147–3145 (1979).
8. K. R. Brownstein, *J. Magn. Reson.*, **40**, 505–510 (1980).
9. D. E. Barnaal and I. J. Lowe, *Phys. Rev. Lett.*, **11**, 258–260 (1963).
10. S. Meiboom and D. Gill, *Rev. Sci. Instr.*, **29**, 688 (1958).
11. H. Y. Carr and E. M. Purcell, *Phys. Rev.*, **94**, 630 (1954).
12. J. R. Vriesenga, S. Chandrasekaran, and P. Luner, *J. Appl. Polym. Sci.*, **37**, 911–921 (1983).
13. L. E. Wise and E. K. Ratliff, *Ann. Chem.*, **19**, 459–462 (1947).
14. B. L. Browning and I. H. Isenberg, in *Wood Chemistry*, 2nd ed., L. E. Wise and E. C. Jahn, Eds., Reinhold, New York, Vol. 2.
15. A. J. Nanassy, *Wood Sci.*, **9**, 104–109 (1976).
16. F. James and M. Roos, *Comput. Phys. Commun.*, **10**, 343–367 (1975).
17. H. J. C. Berendsen, in *Water, A Comprehensive Treatise*, F. Franks, Ed., Plenum, New York, 1975, Vol. 5., pp. 293–330.
18. A. Carrington and A. D. McLachlan, *Introduction to Magnetic Resonance*, Harper and Row, New York, 1967, Chap. 11.
19. J. F. Siau, *Transport Processes in Wood*, Springer-Verlag, Berlin, 1984, pp. 105–112.
20. D. Fengel and G. Wegener, *Wood: Chemistry Ultrastructure, Reactions*, Walter de Gruyter, Berlin, 1983.
21. H. D. Tiemann, *Effect of Moisture Content on the Stiffness of Wood*, U. S. Department of Agriculture Forest Service Bulletin 70, 1906.
22. A. J. Stamm, *Wood and Cellulse Science*, Ronald, New York, 1964.

Received February 25, 1986
Accepted April 18, 1986